Crystal structures of substrate-bound and substrate-free cytochrome P450 46A1, the principal cholesterol hydroxylase in the brain

Natalia Mast*[†], Mark Andrew White[†‡§], Ingemar Bjorkhem[¶], Eric F. Johnson[‖], C. David Stout**[††], and Irina A. Pikuleva*[††]

*Department of Pharmacology and Toxicology, [‡]The Sealy Center for Structural Biology and Molecular Biophysics, and [§]Department of Biochemistry and Molecular Biology, University of Texas Medical Branch, Galveston, TX 77555; [¶]Division of Clinical Chemistry, Karolinska Institute, Huddinge Hospital, S-141 88 Huddinge, Sweden; and [‖]Department of Molecular and Experimental Medicine and **Department of Molecular Biology, The Scripps Research Institute, La Jolla, CA 92037

Communicated by David W. Russell, University of Texas Southwestern Medical Center, Dallas, TX, April 17, 2008 (received for review March 19, 2008)

By converting cholesterol to 24S-hydroxycholesterol, cytochrome P450 46A1 (CYP46A1) initiates the major pathway for cholesterol removal from the brain. Two crystal structures of CYP46A1 were determined. First is the 1.9-Å structure of CYP46A1 complexed with a high-affinity substrate cholesterol 3-sulfate (CH-3S). The second structure is that of the substrate-free CYP46A1 at 2.4-Å resolution. CH-3S is bound in the productive orientation and occupies the entire length of the banana-shaped hydrophobic active-site cavity. A unique helix B′–C loop insertion (residues 116–120) contributes to positioning cholesterol for oxygenation catalyzed by CYP46A1. A comparison with the substrate-free structure reveals substantial substrate-induced conformational changes in CYP46A1 and suggests that structurally distinct compounds could bind in the enzyme active site. *In vitro* assays were performed to characterize the effect of different therapeutic agents on cholesterol hydroxylase activity of purified full-length recombinant CYP46A1, and several strong inhibitors and modest coactivators of CYP46A1 were identified. Structural and biochemical data provide evidence that CYP46A1 activity could be altered by exposure to some therapeutic drugs and potentially other xenobiotics.

cholesterol metabolism | monooxygenase | drug interactions | cholesterol 3-sulfate

Accumulating evidence indicates that neurodegeneration and development of neurological disorders such as Alzheimer's disease (AD) are associated with disturbances in cholesterol homeostasis in the brain (1–5). It is also becoming increasingly clear that the conversion of cholesterol to 24S-hydroxycholesterol (24OH-CH) is an important mechanism that controls cholesterol turnover in the central nervous system (6–8). Cholesterol 24-hydroxylation is carried out by cytochrome P450 46A1 (CYP46A1) and represents the first step in the major pathway for cholesterol elimination from the brain (9–11). Unlike cholesterol, 24OH-CH can cross the blood–brain barrier and be delivered to the liver for further degradation to bile acids.

Studies of CYP46A1-knockout mice indicate that the continued synthesis and turnover of cerebral cholesterol via 24-hydroxylation are necessary for memory and learning (12). There appears to be a link between CYP46A1 and AD; the CYP46A1 expression pattern in the brain and levels of 24OH-CH in the serum and cerebrospinal fluid are different in healthy people and those affected by AD (13–17). The association between polymorphisms in the CYP46A1 gene and susceptibility to AD was also demonstrated in a number of studies (www.alzforum.org). However, this association has not yet been unambiguously proven and is still under investigation. Evidence has also been obtained in cultured cells and mice that supports a role for side-chain oxysterols, including 24OH-CH, as endogenous ligands for liver X receptors, that regulate the expression of genes involved in fatty acid and cholesterol metabolism (7). 24OH-CH was also shown to inhibit the formation of amyloid β-peptides, a hallmark of AD, in cell cultures (14, 18). Additionally, 24OH-CH is thought to induce apolipoprotein E-mediated cholesterol efflux from astrocytes and thus to affect the progression of neurodegenerative diseases, including AD (19).

CYP46A1 is one of the four key enzymes that control cholesterol turnover in mammals (20). All of them belong to the cytochrome P450 superfamily of heme-containing monooxygenases, and all hydroxylate cholesterol, yet at different positions on the sterol molecule (20). CYP7A1 initiates cholesterol degradation in the liver, CYP46A1 in the brain, CYP11A1 in steroidogenic organs, and CYP27A1 in all other tissues. CYP46A1 is the first of these four P450s to be structurally characterized. The substrate-bound and ligand-free crystal structures of human CYP46A1 reveal specific interactions between the enzyme and the high-affinity substrate cholesterol sulfate (CH-3S) and differences between the substrate-bound and substrate-free enzyme conformations. Structural studies suggested that the flexibility of the enzyme might permit the binding of other compounds as substrates or inhibitors, and kinetic experiments identified several marketed drugs that inhibited or stimulated the activity of the enzyme *in vitro*. These results indicate that the activity of CYP46A1 can be modulated by structurally unrelated compounds used as therapeutic agents.

Results and Discussion

Design, Characterization, and Crystallization of a Modified CYP46A1. Crystallographic studies were carried out on Δ(2–50)CYP46A1dH (21), a modified recombinant human CYP46A1, in which the first 50 N-terminal amino acid residues were deleted, and a His_4 tag was added at the C terminus. The truncation removed a 23-residue transmembrane-anchoring domain and rendered this membrane P450 more soluble. These modifications did not adversely affect the kinetic properties of cholesterol, 24OH-CH, and CH-3S hydroxylation (Table 1). Δ(2–50)CYP46A1dH was purified and crystallized in the presence of CH-3S, which we found binds tightly to the enzyme with an estimated K_d of 7 nM,

Author contributions: E.F.J., C.D.S., and I.A.P. designed research; N.M., M.A.W., I.B., and C.D.S. performed research; N.M., M.A.W., I.B., E.F.J., C.D.S., and I.A.P. analyzed data; and M.A.W., E.F.J., C.D.S., and I.A.P. wrote the paper.

The authors declare no conflict of interest.

Data deposition: The atomic coordinates and structure factors have been deposited in the Protein Data Bank, www.pdb.org (PDB ID codes 2Q9F and 2Q9G).

[†]N.M. and M.A.W. contributed equally to this work.

[††]To whom correspondence may be addressed. E-mail: dave@scripps.edu or irpikule@utmb.edu.

This article contains supporting information online at www.pnas.org/cgi/content/full/0803717105/DCSupplemental.

Table 1. Kinetic properties of CYP46A1 against different steroids

CYP4	Cholesterol			24OH-CH			CH-3S		
	k_{cat}, min^{-1}	K_m, μM	k_{cat}/K_m, $min^{-1}/\mu M$	k_{cat}, min^{-1}	K_m, μM	k_{cat}/K_m, $min^{-1}/\mu M$	k_{cat}, min^{-1}	K_m, μM	k_{cat}/K_m, $min^{-1}/\mu M$
Full-length*	0.11†	5.4	0.02	0.92	3.9	0.24	0.46	4.9	0.09
Δ(2–50)*	0.43	7.7	0.06	0.85	1.5	0.56	2.5	3.3	0.8

*Contains a C-terminal His_4 tag, which does not affect the kinetics of hydroxylation.
†The results are means of three to four measurements. SD ≤ 20%.

which is ≈10 times lower than the K_d of the endogenous substrate cholesterol (100 nM). CH-3S is metabolized by both full-length and truncated CYP46A1 reconstituted with cytochrome P450 reductase *in vitro*. The catalytic efficiency of CH-3S hydroxylation by full-length and Δ(2–50)CYP46A1dH was better than that of cholesterol hydroxylation and comparable with the efficiency of 24OH-CH hydroxylation (Table 1). We established that 24OH-CH can be further metabolized by CYP46A1 to 24,25- and 24,27-dihydroxycholesterols in both cell cultures and the *in vitro* reconstituted system (22). Similar to cholesterol (11, 22), the major product in the incubations with CH-3S had a retention time and mass spectrum consistent with hydroxylation at C24 (data not shown). There was also a smaller conversion into a product with a retention time and the mass spectrum indicative of 24,25-dihydroxycholesterol, suggesting sequential hydroxylation of the 24-hydroxycholesterol sulfate. Approximately 10% of 24OH-CH present in human circulation is sulfated (10), and bovine brain contains a similar fraction (≈14%) of sulfated 24OH-CH (23). It is not, however, clear whether sulfated 24OH-CH is formed by the action of CYP46A1 on CH-3S or by the action of a sulfotransferase on 24OH-CH (23). After successful crystallization of the CH-3S–CYP46A1 complex, we crystallized the substrate-free enzyme also.

CH-3S Binding to Δ(2–50)CYP46A1dH. The crystal structure of Δ(2–50)CYP46A1dH complexed with CH-3S was solved (21), and the final model was refined at 1.9-Å resolution [supporting information (SI) Table S1]. CH-3S is not hydroxylated by the enzyme in the crystal structure because it is stable when bound to the ferric form of the P450 in the absence of the electron transfer from P450 reductase. This substrate is positioned unambiguously in the $2|F_o|-|F_c|$ composite-omit map with well defined electron density for the steroid nucleus and carbon atoms C20–C24 of the side chain (Fig. 1*a*). The terminal atoms of the side chain, C25–C27, are less well defined but still within the envelope of the electron density. An increased B-factor for C27 indicates a small rotational vibration or disorder for this methyl group. CH-3S occupies the active-site cavity over its entire length with the steroid side chain facing the distal surface of the heme prosthetic group and the sulfate anion directed toward the protein surface. The sulfate group forms four hydrogen bonds, with His-81 (β1-1–β1-2 loop), Arg-110 (B′ helix), and Asn-227 (F–G loop) of the enzyme (Fig. 1*b*). The steroid nucleus interacts with Phe-80 (β1-1–β1-2 loop), Met-108, Tyr-109, Ala-111, Leu-112 (B′ helix), Ile-222 (F helix), Trp-368, Phe-371 (β1–4 strand), and Ala-474 (β4 loop). Three of these residues, Ala-111, Leu-112, and Ile-222, contact the flat surface of the steroid nucleus; and three, Phe-80, Trp-368, Phe-371, are on the opposite side, contacting the steroid axial methyl groups. Met-108 and Tyr-109 restrain the steroid nucleus along one edge as does Ala-474 at the edge of the C ring. A hydrogen bond between Trp-368 and Ala-474, and a network of hydrogen bonds involving Tyr-109, Thr-370, Phe-371, Arg-372, and a heme propionate position these active-site residues. The aliphatic tail of CH-3S is surrounded by Phe-121, Val-126 (in a B′–C loop insertion, unique to CYP46A1), Ile-301, Ala-302, T306 (I helix), Ala-367 (β4–1 strand), and Thr-475 (β4 loop), which are located at a 3.7- to 4-Å distance and likely to limit its motion. The C24 and C25 atoms of CH-3S, the primary and secondary sites of hydroxylation by CYP46A1, respectively, are positioned at a 5.7 ± 0.05-Å distance from the heme iron (Fig. 1*c*), which is ≈1–1.5 Å greater than expected for hydroxylation by the oxyferryl intermediate during turnover (24). It is likely that CH-3S moves closer to the heme iron during subsequent steps in the catalytic cycle after reduction of the heme iron. The orientation and position of CH-3S suggest that cholesterol will have a similar overall mode of binding. A

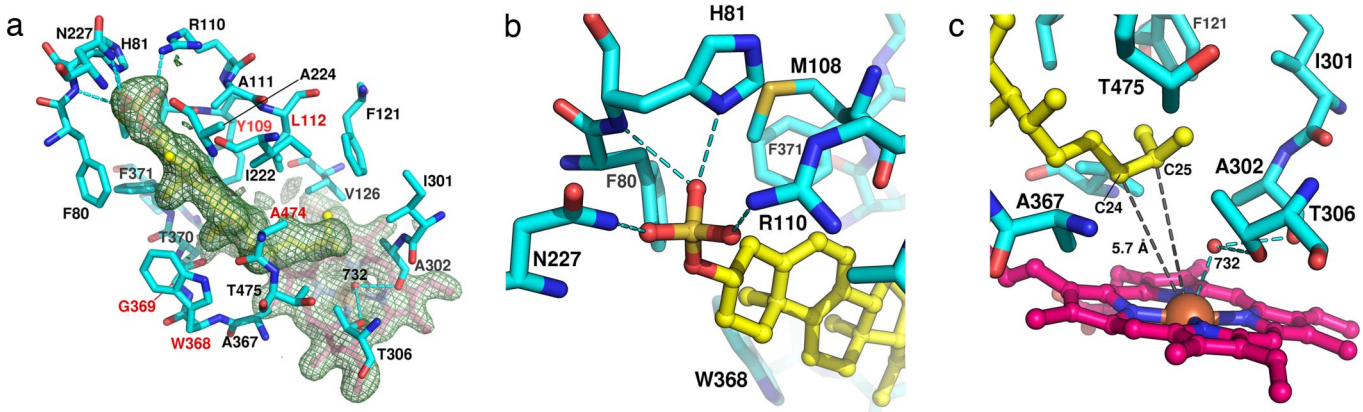

Fig. 1. CYP46A1 active site. (*a*) The composite-omit $2|F_o|-|F_c|$ electron density map (green mesh) contoured at 1.5σ around the heme (in pink) and CH-3S (in yellow). Amino acid residues (in cyan) within 4 Å of CH-3S are shown. The heme iron and water molecule 732 are represented as big brown and small red spheres, respectively. The oxygen, nitrogen, and sulfur atoms are in red, blue, and orange, respectively. Dashed cyan lines indicate hydrogen bonds. Residues forming a circular scaffold are labeled in red. (*b*) Enlarged view of the active site around the sulfate anion of CH-3S and (*c*) in the vicinity of the heme iron. Dashed gray lines connect the C24 and C25 of CH-3S and the heme iron.

BIOCHEMISTRY

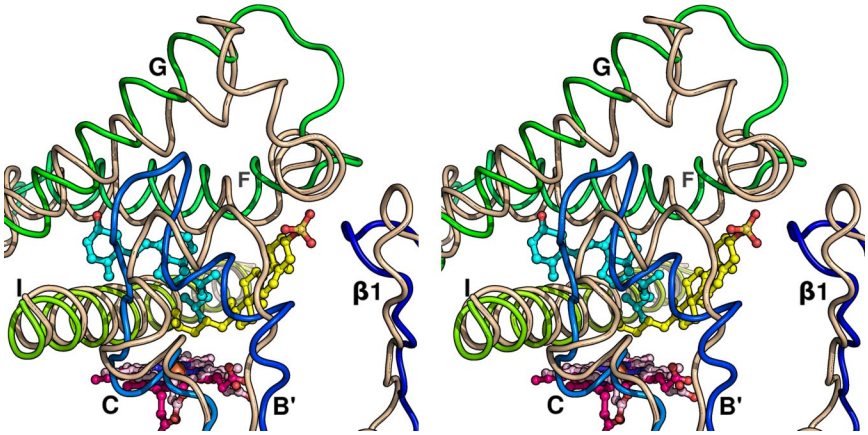

Fig. 2. Superposition of CH-3S-bound CYP46A1 structure (colored from blue at the N terminus to red at the C terminus) and vitamin D_3-bound CYP2R1 structure (in wheat) shown in stereoview. CH-3S and vitamin D_3 are in yellow and cyan, respectively, and heme is in pink in CYP46A1 and in light pink in CYP2R1.

difference could be in contacts of the cholesterol 3β hydroxyl with CYP46A1, and if so, in the depth of insertion in the active site. Residues that may be involved in recognition of the cholesterol 3β hydroxyl are His-81 and Asn-227.

The only other structurally characterized, eukaryotic P450 complexed with the compound similar to cholesterol is vitamin D_3-bound CYP2R1 [Protein Data Bank (PDB) ID code 2OJD].CYP2R1 is a vitamin D 25-hydroxylase (25, 26) that, like CYP46A1, carries out regioselective hydroxylation of the sterol side chain. Several features of the binding of CH-3S exhibit similarities and differences compared with the binding of vitamin D_3 to CYP2R1. Superposition (as described in *Methods*) shows that the two P450s have very different orientations of the substrate with respect to the heme (Fig. 2). In CYP2R1, vitamin D_3 enters the active site between the helices B′, G, and I, whereas in CYP46A1 the entrance to the active-site channel is between the helices B′, F, and the β-1 sheet region. An element that contributes to this difference is the B′–C loop, which contains five extra residues (116–120) in CYP46A1. The B′–C loop is positioned near the G helix in CYP46A1 and blocks substrate access because residues 116–120 extend toward and interact with residues on the G and I helices: in particular, Phe-116–Leu-240; Phe-116 carbonyl–Arg-244; Glu-118–Arg-248; Arg-119–Asp-294, and Leu-120 carbonyl–Arg-251. Conversely in CYP2R1, the β1–4 strand is shifted up to 4 Å, blocking access of vitamin D_3 from the direction observed for CH-3S. Despite the differing routes of substrate access, the structural details in the vicinity of the heme are similar in CYP2R1 and CYP46A1. The C atoms to

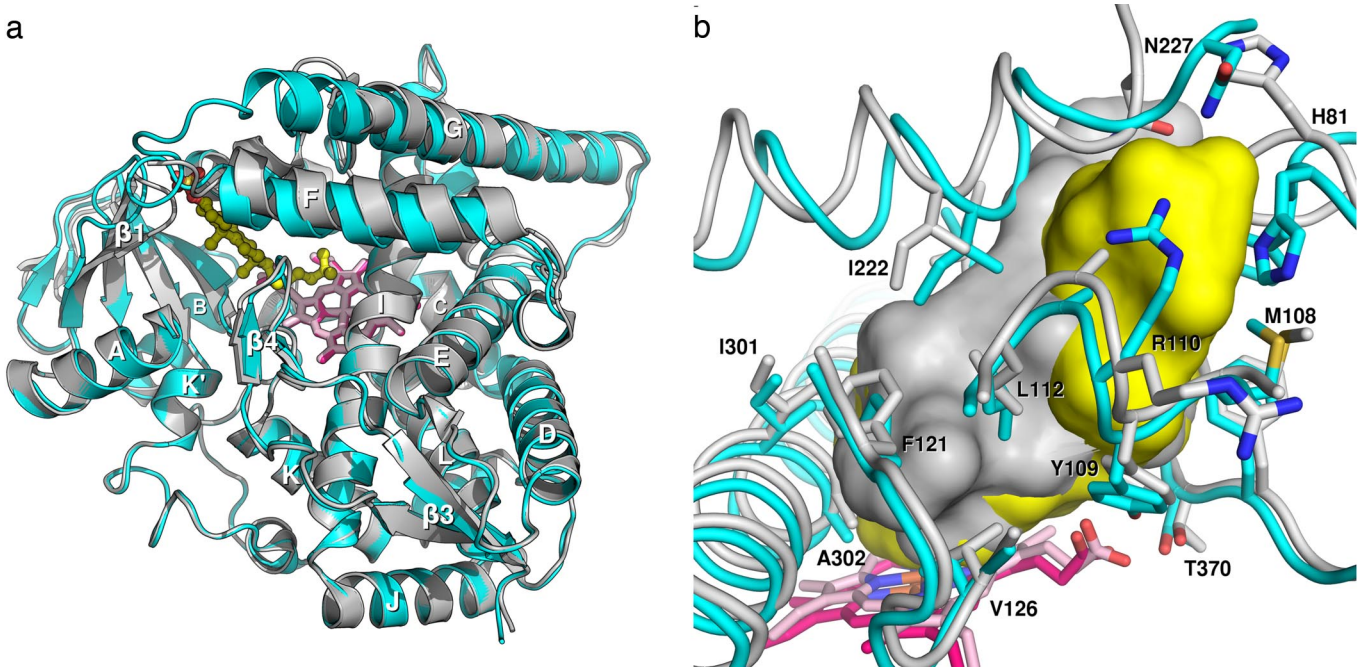

Fig. 3. Comparison of the CH-3S-bound and ligand-free CYP46A1 structures. (*a*) Superposition of the two structures. The CH-3S-bound structure is colored in cyan, heme is in pink, and CH-3S is yellow except for the sulfate group, which is in orange. The ligand-free structure is colored in gray, and heme is in light pink. (*b*) Solvent-accessible surface of the ligand-free (in gray) and CH-3S-bound (in yellow) active sites. The volume does not change significantly from 309 Å^3 in the ligand-free structure to 320 Å^3 in the CH-3S-bound structure as calculated by VOIDOO (27). The active-site residues are colored in gray in the ligand-free structure and in cyan in CH-3S-bound. Side chains in contact with the steroid nucleus shift 0.6–4.2 Å upon substrate binding, whereas residues interacting with the sulfate group shift up to 9–12 Å in the two structures. For clarity, part of the B′–C loop region (residues 113–120) is not displayed.

Table 2. Effect of some drugs and related nonpharmaceuticals on cholesterol hydroxylase activity and binding to CYP46A1

Drug or related compound (indication or use)	Cholesterol hydroxylation, %	K_d, nM
No additive	100 ± 4	
Cholesterol	27 ± 3	100 ± 12
Clobenpropit (experimental anticonvulsant)	ND*	80 ± 9
Thioperamide (experimental anticonvulsant)	34 ± 4	50 ± 10
Tranylcypromine (antidepressant)	ND	7 ± 2
Phenacetin (first nonsteroidal antiinflammatory drug)	135 ± 5	
Acetaminophen (active ingredient of Tylenol)	132 ± 4	
4′-(2-Hydroxyethoxy)-acetanilide	145 ± 9	
Quinine (antimalarial)	112 ± 5	
Quinidine (antiarrhythmic)	68 ± 4	
Lansoprazole (proton pump inhibitor)	86 ± 5	
Dapsone (antibacterial)	89 ± 6	

*ND, not detectable. The results are means of quadruple experiments.

be hydroxylated in the CH-3S and vitamin D_3 side chains (C24 and C25, respectively) are at similar distances from the heme iron (5.7 Å and 6.4 Å, respectively), and the substrate side chains are oriented at virtually identical angles relative to the plane of the heme. In both enzymes, substrate selectivity largely reflects interactions with the protein near the entrance of the substrate-binding site where the sterol and secosterol portions of each molecule are sequestered.

Ligand-Free CYP46A1 Structure Compared with the Substrate-Bound Form. The crystal structure of ligand-free Δ(2–50)CYP46A1dH was solved and refined at 2.4-Å resolution. Major differences in the substrate-bound vs. unliganded structures are observed in the positions of the secondary structure elements that define the entrance to the active-site cavity, helices B′ and F (residues 106–113 and 209–225, respectively), and the loop linking sheets β1-1 and β1-2 (residues 79–83) (Fig. 3*a*). Binding of CH-3S induces concerted movement of helix B′ and the F–G loop inward and the β1-1–β1-2 loop outward. These movements are accompanied by shortening of the sheets β1-1 and β1-2 and elongation of the G helix by 1.5 turns, which together with the F helix, also shifts toward the β-sheet domain. The F–G loop becomes more stabilized in the CH-3S structure and could be traced; in the substrate-free structure electron density for residues 230–239 is not observed. Substrate binding results in a formation of the channel that extends ≈25 Å from the heme Fe to the protein surface. Although the shape of the active-site cavity changes when CH-3S binds (Fig. 3*b*), the volume of the active site does not change appreciably as calculated by VOIDOO (27). The second group of residues affected by conformation changes in CYP46A1 comprises five active-site residues that restrain the steroid nucleus around the C–D ring junction (Tyr-109, Leu-112, Trp-368, Gly-369, and Ala-474; Figs. 1*a* and 3b). These residues form a circular scaffold and shift inward upon interaction with the substrate. They are connected to the residues at the entrance to the active site via a network of hydrogen bonds. It is possible that conformational changes on the CYP46A1 surface and the substrate-induced constriction of the internal circular scaffold are coordinated.

Water plays an important role in P450 catalysis by providing protons. In the ligand-free structure, the heme-coordinating water, W718, is located 2.35 Å from the Fe (Fig. S1). Binding of CH-3S displaces this water molecule ≈0.8 Å parallel to the heme plane to the position of W732. The distance to Fe increases to 2.87 Å, and W732 becomes hydrogen-bonded to Thr-306 (2.9 Å) and Ala-302 (2.9 Å). The proximity of W732 to the heme iron could explain the partial low-to-high spin conversion in Δ(2–50)CYP46A1dH when CH-3S binds.

Pharmacological Implications of the CYP46A1 Structures. Conformational flexibility of the active site suggested a potential for the enzyme to accommodate ligands other than sterols. This prompted an evaluation of the inhibitory properties of >50 compounds (Table S2), both marketed drugs and nonpharmaceuticals, in an assay employing a fixed concentration of cholesterol as a substrate (2.7 μM, equal to 0.5 K_m), and fixed concentration of the potential inhibitor (43 μM). Data on only three compounds, the CNS active drugs clobenpropit, thioperamide, and tranylcypromine, which had a significant inhibitory effect on CYP46A1 under the experimental conditions used are shown in Table 2. No cholesterol hydroxylase activity was detected in the incubations with clobenpropit and tranylcypromine, and inhibition with thioperamide was 66%. All three drugs elicited a spectral response in CYP46A1, permitting determination of their apparent K_d values. The binding affinities of these compounds were in the low nanomolar range and thus in agreement with the observed significant inhibition of the CYP46A1 activity. Because the drug-induced difference spectra were of a type II response, which occurs when the heme-coordinating water is substituted by a nitrogen atom (28, 29), the determined K_d values should correlate well with the IC_{50} values, as established by previous studies of other P450s (30). Information on pharmacokinetics of tranylcypromine in humans is available. The peak plasma concentrations of tranylcypromine lie in the 0.065–0.19 μg/ml (0.49–1.43 μM) range (31), indicating that it has a potential to inhibit CYP46A1 *in vivo*.

Perhaps more exciting was a discovery that three compounds modestly activate cholesterol hydroxylation by CYP46A1. Cholesterol 24-hydroxylation was increased by >30% in the presence of phenacetin or acetaminophen (Table 2). Subsequent testing of nine nonpharmaceutical analogs of phenacetin (Table S2) and some of the known P450 activators (quinine, quinidine, lansoprazole, and dapsone) led to identification of an additional activator. The phenacetin analog, 4′-(2-hydroxyethoxy)-acetanilide, caused even greater, 45%, stimulation of the cholesterol hydroxylase activity of CYP46A, whereas quinine, quinidine, lansoprazole, and dapsone modestly inhibited CYP46A1 (Table 2). Although a larger activation would probably be required to affect cholesterol turnover significantly *in vivo*, the current results serve as a proof of concept that activation of CYP46A1 is possible, in principle. The mechanism for this activation could be similar to that proposed for the stimulation of the CYP2C9-mediated 4′-hydroxylation of flurbiprofen by dapsone (32–34). The stimulation is suggested to occur via simultaneous binding of dapsone and flurbiprofen to the active site of CYP2C9 with dapsone binding limiting the motion of flurbiprofen and affecting the hydration of the active site. There is an unfilled space, or a subpocket, in the active site of CH-3S-bound CYP46A1 (Fig. S2). The subpocket is adjacent to the CH-3S side chain and delimited by segments of the I helix (Ile-301) and F helix (Val-215, Ile-219, Ile-222), the loop between the β4-1 and β4-2 strands (Ala-474), and a part of the B′–C loop (Leu-112, Leu-120, Phe-121). This void could serve as a site for binding of small xenobiotics in the presence of cholesterol, where they might influence the position of the aliphatic tail of the cholesterol to improve the efficiency of hydroxylation. Although this subpocket is small, it increases in size if the substrate moves closer to the heme during activation occurring throughout optimization of the substrate position for reaction. Additionally, the insertion in the helix B′–C loop is likely to be sufficiently malleable to deform in the presence of the

BIOCHEMISTRY

activator because it exhibits a loop structure as seen in the rearrangement upon CH-3S binding. The other possibility is that the coactivators exert their effect through some other mechanism that does not involve the subpocket.

In summary, this work demonstrates crystallization of a human enzyme that utilizes cholesterol as a primary endogenous substrate. The enzyme is distantly related to other structurally characterized mammalian P450s. The two CYP46A1 structures indicate that binding of CH-3S elicits an induced fit that serves to anchor the cholesterol nucleus near the active-site entrance and restrict the motion of the aliphatic side chain near the catalytic center of the molecule. The flexibility of the protein may render the enzyme susceptible to inhibition/stimulation by structurally unrelated compounds as demonstrated by the identification of several inhibitors and activators of cholesterol 24-hydroxylation among a panel of drugs used in clinical practice.

Methods

Protein Purification and Crystallization. CYP46A1 complexed with CH-3S was expressed, purified, and crystallized as described in ref. 21. The substrate-free form was purified by using the same protocol as the CH-3S-bound form except that the substrate was omitted from all of the buffers, and 30 mM histidine was used to elute the enzyme from the Ni–agarose column. Crystals of substrate-free CYP46A1 were obtained under conditions similar to those of the CH-3S-bound CYP46A1, by microseeding with a cat whisker (21). The well solution was 8% PEG 8000, 50 mM potassium phosphate buffer (KP_i), pH 4.7, 20% (vol/vol) glycerol.

Structure Determination and Refinement. The CH-3S-bound structure was solved by using MIRAS data collected in-house as described in ref. 21 and then refined by using high-resolution data (Table S1). The high-resolution data were collected at the Stanford Synchrotron Radiation Laboratory (SSRL) beam line BL 11-1, with 0.97945-Å radiation. The same beam line was used to collect a high-resolution dataset from a substrate-free CYP46A1 crystal. The structure of substrate-free CYP46A1 was solved by rigid-body refinement with the CH-3S-bound CYP46A1 structure as a starting model. Both structures were refined by using PMB/CNS (35, 36). The quality of each structure was assessed by using Molprobity (37). The CH-3S-bound structure had 97.9% residues in the most favored region, 2.1% in the allowed region, and no outliers. Similarly, the substrate-free structure had 95.9% of residues in the favored region, 4.1% in the allowed region and no outliers.

Spectral Binding Studies. Binding affinities of different compounds were estimated as described (22, 38) by using 0.25 μM P450. Titrations of Δ(2–50)CYP46A1dH were carried out in 50 mM KP_i, pH 7.2, containing 50 mM NaCl; the assay buffer for full-length CYP46A1 contained 100 mM NaCl and 0.02% Cymal-6. Steroids were added from 0.2–5 mM stocks in 2.5–45% aqueous 2-hydroxypropyl-β-cyclodextrin; clobenpropit, thioperamide, phenacetin, acetaminophen, 4′-(2-hydroxyethoxy)-acetanilide, quinine, quinidine, lansoprazole, and dapsone were dissolved in water, and tranylcypromine in 50% MetOH. The K_d and maximal absorbance change were estimated by nonlinear least-squares fitting by using the quadratic form of the single-site binding equation (39).

Kinetic Studies. The ability of recombinant CYP46A1 to metabolize CH-3S was tested by using CYP46A1 reconstituted with cytochrome P450 reductase *in vitro*. After termination of the enzyme reaction, the substrate and products were extracted, solvolyzed, converted into trimethylsilyl ethers, and analyzed by gas chromatography-mass spectrometry as described in ref. 22. Kinetic parameters for cholesterol, 24OH-CH, and CH-3S were determined at 37°C in detergent-free 50 mM KP_i containing 50 mM NaCl, if Δ(2–50)CYP46A1dH was used, or in the presence of 40 μg of dilauroylglycerol-3-phosphatidylcholine, 100 mM NaCl, and 0.02% Cymal-6, if full-length CYP46A1 was used. The reaction conditions were optimized for the formation of only one product. The reconstituted system (1 ml) contained 0.1–0.25 μM P450, 0.5 μM NADPH cytochrome P450 oxidoreductase, varying concentrations of cold substrate (1–75 μM), 250,000 cpm of radiolabeled substrate, and 2 units of catalase. The enzymatic reaction was initiated by 1 mM NADPH, carried out for 5–15 min, and terminated by vortexing with 2 ml of CH_2Cl_2, if cholesterol or 24OH-CH was used, or with butanol containing 0.3 M NaCl, if CH-3S was used. The organic phase was isolated, evaporated, dissolved in acetonitrile, and subjected to HPLC. Incubations with cholesterol and 24OH-CH were separated as described in ref. 38 and those with CH-3S by using a linear gradient between solvent A (CH_3OH:CH_3CN:H_2O, 40:10:50, vol/vol) and solvent B (100% CH_3OH) over 15 min, after which the flow was kept at 100% solvent B for another 7 min. Substrate metabolism was $<$18% and linear with reaction time and enzyme concentration. Data were analyzed as described in ref. 22.

Inhibition/Stimulation Studies. The effects of different compounds on cholesterol hydroxylase activity of CYP46A1 were evaluated in the reconstituted system comprising 0.25 μM full-length recombinant CYP46A1, 0.5 μM NADPH cytochrome P450 oxidoreductase, 2.7 μM cholesterol as a substrate, trace amounts of [^{3}H]cholesterol (250,000 cpm), and 43 μM test compound. The assay buffer was the same as in kinetic studies.

Alignment of P450s. Sequences of 12 structurally characterized mammalian P450s (PDB ID codes 1Z10, 2P85, 1SU0, 1PQ2, 1R90, 1NR6, 2F9Q, 20JD, 2HI4, 1TQN, 2Q9F, and 2IAG) were aligned by using ClustalW (Fig. S3). From this alignment, six blocks of 238 residues throughout the protein sequence that do not have any insertions or deletions in any of the 12 were identified. For each structure, the α-carbons (C^α) of these residues were used for alignment with CYP46A1 by using the MIFit least-squares fit function (J. Badger and D. E. McRee, Active Sight). The rmsd for the 238 C^α atoms used in the alignment of CYP46A1 and CYP2R1 is 3.0 Å.

ACKNOWLEDGMENTS. We thank the Stanford Synchotron Radiation Laboratory (SSRL) staff for their generous assistance. SSRL is a national user facility operated by Stanford University on behalf of the U.S. Department of Energy, Office of Basic Energy Sciences. The SSRL Structural Molecular Biology Program is supported by the Department of Energy, Office of Biological and Environmental Research, and by the National Institutes of Health, National Center for Research Resources, Biomedical Technology Program, and the National Institute of General Medical Sciences. We also thank Dr. K. Johnson and Dr. J. Gallagher (University of Texas Medical Branch, Galveston, TX) for providing some of the drugs tested in this work. The work was supported by National Institutes of Health Grants GM62882, AG024336, EY018383 (to I.A.P.) and GM031001 (to E.F.J.) and by grants from the Swedish Science Council and Brain Power (to I.B.), Merck Research Laboratories (to I.A.P.), the Sealy and Smith Foundation (to I.A.P. and to the Sealy Center for Structural and Molecular Biology at University of Texas Medical Branch).

1. Dietschy JM, Turley SD (2001) Cholesterol metabolism in the brain. *Curr Opin Lipidol* 12:105–112.
2. Bjorkhem I, Meaney S (2004) Brain cholesterol: Long secret life behind a barrier. *Arterioscler Thromb Vasc Biol* 24:806–815.
3. Wolozin B (2004) Cholesterol and the biology of Alzheimer's disease. *Neuron* 41:7–10.
4. Reiss AB (2005) Cholesterol and apolipoprotein E in Alzheimer's disease. *Am J Alzheimer's Dis Other Demen* 20:91–96.
5. Carter CJ (2007) Convergence of genes implicated in Alzheimer's disease on the cerebral cholesterol shuttle: APP, cholesterol, lipoproteins, and atherosclerosis. *Neurochem Int* 50:12–38.
6. Bjorkhem I (2006) Crossing the barrier: Oxysterols as cholesterol transporters and metabolic modulators in the brain. *J Intern Med* 260:493–508.
7. Chen W, Chen G, Head DL, Mangelsdorf DJ, Russell DW (2007) Enzymatic reduction of oxysterols impairs LXR signaling in cultured cells and the livers of mice. *Cell Metab* 5:73–79.
8. Lutjohann D (2006) Cholesterol metabolism in the brain: Importance of 24S-hydroxylation. *Acta Neurol Scand Suppl* 185:33–42.
9. Bjorkhem I, *et al*. (1998) Cholesterol homeostasis in human brain: Turnover of 24S-hydroxycholesterol and evidence for a cerebral origin of most of this oxysterol in the circulation. *J Lipid Res* 39:1594–1600.
10. Lutjohann D, *et al*. (1996) Cholesterol homeostasis in human brain: Evidence for an age-dependent flux of 24S-hydroxycholesterol from the brain into the circulation. *Proc Natl Acad Sci USA* 93:9799–9804.
11. Lund EG, Guileyardo JM, Russell DW (1999) cDNA cloning of cholesterol 24-hydroxylase, a mediator of cholesterol homeostasis in the brain. *Proc Natl Acad Sci USA* 96:7238–7243.
12. Kotti TJ, Ramirez DM, Pfeiffer BE, Huber KM, Russell DW (2006) Brain cholesterol turnover required for geranylgeraniol production and learning in mice. *Proc Natl Acad Sci USA* 103:3869–3874.
13. Bogdanovic N, *et al*. (2001) On the turnover of brain cholesterol in patients with Alzheimer's disease: Abnormal induction of the cholesterol-catabolic enzyme CYP46 in glial cells. *Neurosci Lett* 314:45–48.
14. Brown J, III, *et al*. (2004) Differential expression of cholesterol hydroxylases in Alzheimer's disease. *J Biol Chem* 279:34674–34681.
15. Lutjohann D, *et al*. (2000) Plasma 24S-hydroxycholesterol (cerebrosterol) is increased in Alzheimer and vascular demented patients. *J Lipid Res* 41:195–198.
16. Schonknecht P, *et al*. (2002) Cerebrospinal fluid 24S-hydroxycholesterol is increased in patients with Alzheimer's disease compared with healthy controls. *Neurosci Lett* 324:83–85.

17. Kolsch H, *et al*. (2004) Altered levels of plasma 24S- and 27-hydroxycholesterol in demented patients. *Neurosci Lett* 368:303–308.
18. Famer D, *et al*. (2007) Regulation of α- and β-secretase activity by oxysterols: Cerebrosterol stimulates processing of APP via the α-secretase pathway. *Biochem Biophys Res Commun* 359:46–50.
19. Abildayeva K, *et al*. (2006) 24(S)-hydroxycholesterol participates in a liver X receptor-controlled pathway in astrocytes that regulates apolipoprotein E-mediated cholesterol efflux. *J Biol Chem* 281:12799–12808.
20. Pikuleva IA (2006) Cholesterol-metabolizing cytochromes P450. *Drug Metab Dispos* 34:513–520.
21. White MA, *et al*. (2008) Use of complementary cation and anion heavy atom salt derivatives used to solve the structure of cytochorme P450 46A1. *Acta Crystallogr D* 64:487–495.
22. Mast N, *et al*. (2003) Broad substrate specificity of human cytochrome P450 46A1 which initiates cholesterol degradation in the brain. *Biochemistry* 42:14284–14292.
23. Prasad VV, Ponticorvo L, Lieberman S (1984) Identification of 24-hydroxycholesterol in bovine adrenals in both free and esterified forms and in bovine brains as its sulfate ester. *J Steroid Biochem* 21:733–736.
24. Poulos TL, Johnson EF (2005) *Structures of Cytochrome P450 Enzymes*, Ortiz de Montellano PR, ed (Kluwer, New York), 3rd Ed, pp 87–114.
25. Cheng JB, Motola DL, Mangelsdorf DJ, Russell DW (2003) De-orphanization of cytochrome P450 2R1: A microsomal vitamin D 25-hydroxylase. *J Biol Chem* 278:38084–38093.
26. Cheng JB, Levine MA, Bell NH, Mangelsdorf DJ, Russell DW (2004) Genetic evidence that the human CYP2R1 enzyme is a key vitamin D 25-hydroxylase. *Proc Natl Acad Sci USA* 101:7711–7715.
27. Kleywert GJ, Jones TA (1994) Detection, delineation, measurement and display of cavities in macromolecular structures. *Acta Crystallogr D* 50:178–185.
28. Dawson JH, Andersson LA, Sono M (1982) Spectroscopic investigations of ferric cytochrome P-450–CAM ligand complexes: Identification of the ligand trans to cysteinate in the native enzyme. *J Biol Chem* 257:3606–3617.
29. Poulos TL, Howard AJ (1987) Crystal structures of metyrapone- and phenylimidazole-inhibited complexes of cytochrome P-450cam. *Biochemistry* 26:8165–8174.
30. Murray M, Wilkinson CF (1984) Interactions of nitrogen heterocycles with cytochrome P-450 and monooxygenase activity. *Chem Biol Interact* 50:267–275.
31. Mallinger AG, Edwards DJ, Himmelhoch JM, Knopf S, Ehler J (1986) Pharmacokinetics of tranylcypromine in patients who are depressed: Relationship to cardiovascular effects. *Clin Pharmacol Ther* 40:444–450.
32. Hutzler JM, Hauer MJ, Tracy TS (2001) Dapsone activation of CYP2C9-mediated metabolism: Evidence for activation of multiple substrates and a two-site model. *Drug Metab Dispos* 29:1029–1034.
33. Wester MR, *et al*. (2004) The structure of human cytochrome P450 2C9 complexed with flurbiprofen at 2.0-A resolution. *J Biol Chem* 279:35630–35637.
34. Locuson CW, Gannett PM, Ayscue R, Tracy TS (2007) Use of simple docking methods to screen a virtual library for heteroactivators of cytochrome P450 2C9. *J Med Chem* 50:1158–1165.
35. Scott EE, *et al*. (2004) Structure of mammalian cytochrome P450 2B4 complexed with 4-(4-chlorophenyl)imidazole at 1.9-A resolution: Insight into the range of P450 conformations and the coordination of redox partner binding. *J Biol Chem* 279:27294–27301.
36. Brunger AT, *et al*. (1998) Crystallography and NMR system: A new software suite for macromolecular structure determination. *Acta Crystallogr D* 54:905–921.
37. Lovell SC, *et al*. (2003) Structure validation by C^{α} geometry: Phi, psi and C^{β} deviation. *Proteins* 50:437–450.
38. Mast N, Andersson U, Nakayama K, Bjorkhem I, Pikuleva IA (2004) Expression of human cytochrome P450 46A1 in *Escherichia coli*: Effects of N- and C-terminal modifications. *Arch Biochem Biophys* 428:99–108.
39. Copeland RA (2000) Protein-ligand binding equilibria, in *The Enzymes*, Copeland RA, ed (Wiley, New York), 2nd Ed, pp 76–108.